Vacuum 167 (2019) 397–406

Contents lists available at ScienceDirect

Vacuum

journal homepage: www.elsevier.com/locate/vacuum

Temperature-controlled growth of micro- and nanocrystals on the surface of NiO + CuO/TiO_2/Ti composites

V.S. Rudnev[a,b,*], I.V. Lukiyanchuk[a], M.S. Vasilyeva[b], T.A. Kaidalova[a]

[a] Institute of Chemistry of Far Eastern Branch of Russian Academy of Sciences, Vladivostok, Russia
[b] Far Eastern Federal University, Vladivostok, Russia

ARTICLE INFO

Keywords:
Titanium
Plasma electrolytic oxidation
Impregnating
Air annealing
Surface architecture
Micro- and nanocrystals

ABSTRACT

The functional properties of oxide coatings on metals depend on the composition and structure of their surface. In this work, the change with temperature of air annealing of the surface of NiO + CuO/TiO_2/Ti composites formed by the combination of plasma electrolytic oxidation of titanium in the phosphate-borate-tungstate electrolyte containing nickel and copper acetates and impregnation in the solution of nickel and copper nitrates was studied. It has been shown that varying the annealing temperature allows one to form the ensembles of micro- and nano-sized crystals of different composition and structure on the surface. CuO crystals are formed on the surface at annealing temperature T = 500 ÷ 700 °C, $NiWO_4$ crystals are present at T = 750 ÷ 850 °C, and $Ni_{2.62}Ti_{0.69}O_4$ whiskers - at T ≥ 900 °C. The data obtained suggest that the remaining electrolyte and impregnating solution accumulated on the surface and in the pores, as well as the transport of titanium from the coating depth to the surface, play an important role in the formation of crystals. It was summarized that air annealing at given temperatures of complex oxide coatings can be effective for controlling their architecture and surface composition at the micro- and nanolevels and, therefore, their functional properties.

1. Introduction

Oxide coatings on titanium, aluminum or magnesium, formed in electrolytes under spark and/or microarc electrical discharges, are already used as protective [1,2] and biocompatible ones [3,4]. They are also promising for use in catalysis [5,6], sensorics [7,8], heat absorption or scattering [9,10], as materials with certain magnetic [11,12] or optical characteristics [13,14]. The formation technique, including parallel electrochemical and plasma-thermal processes, is called plasma electrolytic or microarc oxidation (PEO or MAO) [15–21]. One of the scientifically and practically significant features of PEO is the possibility of forming the coatings of a certain oxide composition and, therefore, of a specific purpose by varying the electrolyte composition and the processing conditions [16,17,22,23].

The properties of PEO-coatings depend on many factors, including the composition and architecture of their surface. The search for ways of controlling these characteristics opens up new additional possibilities for obtaining coatings for various purposes.

A number of publications have noted that micro- and nanoformations are present on the surface of oxide coatings already after PEO [24–29] in electrolytes of complex composition. However, the processes and conditions of their formation during the PEO, as well as the ability to control their composition remain poorly understood.

The use of additional post treatment opens up more possibilities for controlling the composition and surface structure of PEO coatings at micro- and nanolevels [29–44]. For example, after chemical treatment in alkaline solution, the surface of the PEO coatings on titanium was transformed into a 3D nano-flaky surface network. The obtained nanoflakes were around 100–200 nm in dimension, with a flake thickness of less than 10 nm [32]. Such composites with large surface area are promising for use in solar energy converters. Hydrothermal treatment of titanium-supported PEO coatings containing calcium hydroxyapatite in aqueous alkaline solution made it possible to form ensembles of hydroxyapatite nanocrystals on their surface [33,34]. The latter significantly improved the interaction of the surface of titanium implants with biological tissues. Cathodic processing the PEO-coated titanium samples with the high-voltage pulse in the sulphuric acid solution containing $CdSO_4$ and H_2SeO_3 was used for deposition of CdSe micro- and nanoparticles onto their surface [35]. The application of organic paste with $Bi(NO_3)_3$ to PEO-coated samples of TiO_2/Ti and subsequent air annealing at 700 °C led to the formation of regular micro- and nanocrystals of bismuth titanate $Bi_4Ti_3O_{12}$ in the outer layer [36]. CdSe/TiO_2/Ti and $Bi_4Ti_3O_{12}$/TiO_2/Ti composites are of interest for testing as photocatalysts. The deposition of titanium hydroxide gel with

* Corresponding author. Institute of Chemistry of Far Eastern Branch of Russian Academy of Sciences, Vladivostok, Russia.
E-mail address: rudnevvs@ich.dvo.ru (V.S. Rudnev).

https://doi.org/10.1016/j.vacuum.2019.06.039
Received 19 April 2019; Received in revised form 23 May 2019; Accepted 29 June 2019
Available online 29 June 2019
0042-207X/

palladium nanoparticles stabilized by micelles of a siloxane-acrylate emulsion on $SiO_2/TiO_2/Ti$ samples and subsequent annealing resulted in the formation of the composites with disperse palladium particles about 25–60 nm in size anchored on the surface [37]. At a low palladium concentration on the surface (0.04–0.2 at.%), the formed composites catalyzed the oxidation of CO into CO_2 at temperatures above 170 °C.

A combination of PEO and impregnation followed by air annealing opens up the interesting possibilities in obtaining the surfaces extended at micro- and nanolevels [38–43]. In Ref. [29], NiO + CuO/PEO-layer/Ti composites containing up to 20 at. % Ni and 20 at. % Cu were formed by combination of PEO technique in the PBWNiCu electrolyte (Na_3PO_4 + $N_2B_4O_7$ + Na_2WO_4 + $Ni(CH_3COO)_2$ + Cu $(CH_3COO)_2$) and impregnation in solution of $Ni(NO_3)_2$ + Cu $(NO_3)_2$ followed by air annealing at 500°C. The composites catalyzed the reaction of oxidation of CO to CO_2 at temperatures above 200 °C. After annealing at 700 °C, individual nanowhiskers appeared at the surface of such composites in and around the pores, and after annealing at temperatures above 850 °C, the brushes of nanowhiskers of the supposed composition of Ni_5TiO_7 occupied a significant coating surface [38,39]. Such samples lost their activity in CO oxidation [38], but acquired the ability to catalyze the destruction of naphthalene that was analogue of tar in biomass gasification [39]. This approach was developed in Refs. [41–43], in which the composites with ensembles of nanowhiskers, nanoplates, nanowires, nanorods and nanosheets of $NiWO_4$ or $ZnWO_4$ (annealing at T = 650–850 °C) [40], $MnWO_4$, (annealing at 650–850 °C) [41], $(Ni_{1-x}Co_x)_5TiO_7$ (annealing at 1050°C) [43] were obtained. Moreover, in Refs. [41,43], the operation of additional impregnation was excluded. Such surface transformation gives functional properties to the composites. Composites with nanocrystals of $NiWO_4$, $ZnWO_4$ and $MnWO_4$ exhibited photocatalytic activity [40,41], and those with $Ni(Ni_{1-x}Co_x)_5TiO_7$ nanowhiskers catalized the oxidation of CO into CO_2 [43].

Comparing the results of works [40,42], one can find that crystals of different nature are formed on the surface of $NiO/TiO_2/Ti$ composites when using the electrolytes of similar composition for PEO and the same impregnating solutions, but different annealing temperatures. For example, $NiWO_4$ nanocrystals and Ni_5TiO_7 nanowhiskers were formed as a result of annealing at 850 °C and 1050°C, respectively. In addition, from the data of [38], it follows that with increasing annealing temperature, as to XPS, the elemental compositions of NiO + $CuO/TiO_2/Ti$ surfaces change, and their activities in CO oxidation decrease. These facts indicate that not only the elemental composition, but also the surface architecture at micro- and nanolevels depend on the annealing temperature, which was experimentally confirmed in Ref. [44].

In this work, we studied the effects of the annealing temperature on the phase composition of NiO + $CuO/TiO_2/Ti$ composites and impact of impregnating solution concentrations on the morphology of the coating surfaces. Using the data of work [44] and new results, we analyzed for the first time the regularities of the growth of micro- and nanocrystals on the surface of NiO + $CuO/TiO_2/Ti$ composites and made assumptions about the possible mechanisms of these processes.

2. Experimental

2.1. Sample preparation

PEO layers were formed on the samples from wire with a diameter of 2 mm and a length of 16 cm and on flat plates of 20 × 20 × 1 mm in size from VT1-0 technical titanium (Ti content is above 99.6%, grade 2). Flat samples were used for X-ray diffraction patterns and wire ones – for surface morphology studies. This separation is associated with the following considerations: (1) previous studies [38,39] were carried out with wire samples, (2) coatings on wires are more resistant to mechanical manipulations, such as cutting, especially after high-temperature annealing, (3) high-quality X-ray patterns are difficult to obtain on wire samples.

Before oxidation, to standardize the surface, the samples were chemically polished to a mirror gloss (8–9 grade) in a mixture of HF: HNO_3 = 1: 3 (by volume) at 70 °C. Then PEO-coated samples were washed with distilled water and dried in air at 70 °C.

Ni-, Cu-containing PEO coatings on titanium were formed, as in Refs. [29,38,39,44], in an aqueous PBWNiCu electrolyte containing, mol/L: 0.066 Na_3PO_4 + 0.034 $Na_2B_4O_7$ + 0.006 Na_2WO_4 + 0.1 Ni $(CH_3COO)_2$ + 0.025 $Cu(CH_3COO)_2$, at anodic polarization with an effective current density of i = 0.1 A/cm^2 for 10 min. The current source was computer-controlled TER4-100/460 thyristor unit (Russia) operating in unipolar mode. The counter electrode was stainless steel bath body with a water-cooling jacket. The electrolyte was stirred using a mechanical stirrer. The electrolyte temperature did not exceed 30 °C during PEO.

The PEO-coated samples were immersed in an aqueous solution containing 1 mol/L Cu $(NO_3)_2$ and 1 mol/L $Ni(NO_3)_2$. The compositions were kept in an impregnating solution for 1 h. Thereafter, the samples were dried over an electric heater in air and annealed in a furnace at 500°C for 4 h. The annealing temperature similar to that used in Refs. [29,38,39,44] allows one to completely decompose the nitrates. The scheme for obtaining the initial samples is presented in Fig. 1. Note, that in some cases higher 2 mol/L Cu $(NO_3)_2$ + 2 mol/L $Ni(NO_3)_2$ or lower 0.5 mol/L Cu $(NO_3)_2$ + 0.5 mol/L $Ni(NO_3)_2$ concentrations of impregnating solutions were used. These cases will be discussed separately.

Hereafter, the wire sample with initial coating was cut into pieces of length of 1.5 cm. These individual pieces, as well as flat samples with similar coatings, were additionally annealed in air for 4 h at one of the set temperatures: 700, 750, 800, 850, 900, 950, or 1050 °C. That is, the each individual sample has been additionally annealed only at one temperature.

All manipulations, including PEO treatment, impregnation and air annealing, are performed at a pressure of 1 atm.

2.2. Structural and composition characterization

The surface morphology was studied using a high resolution Hitachi S5500 (Japan) scanning electron microscope (SEM) equipped with an Ultra Dry energy dispersive spectrometer (Thermo Scientific, USA). To

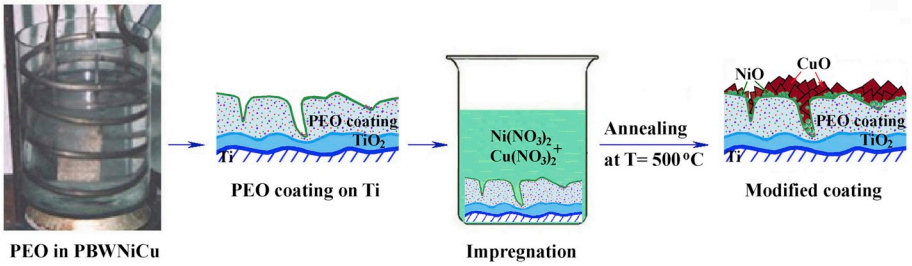

Fig. 1. Scheme for obtaining the modified NiO + $CuO/TiO_2/Ti$ samples.

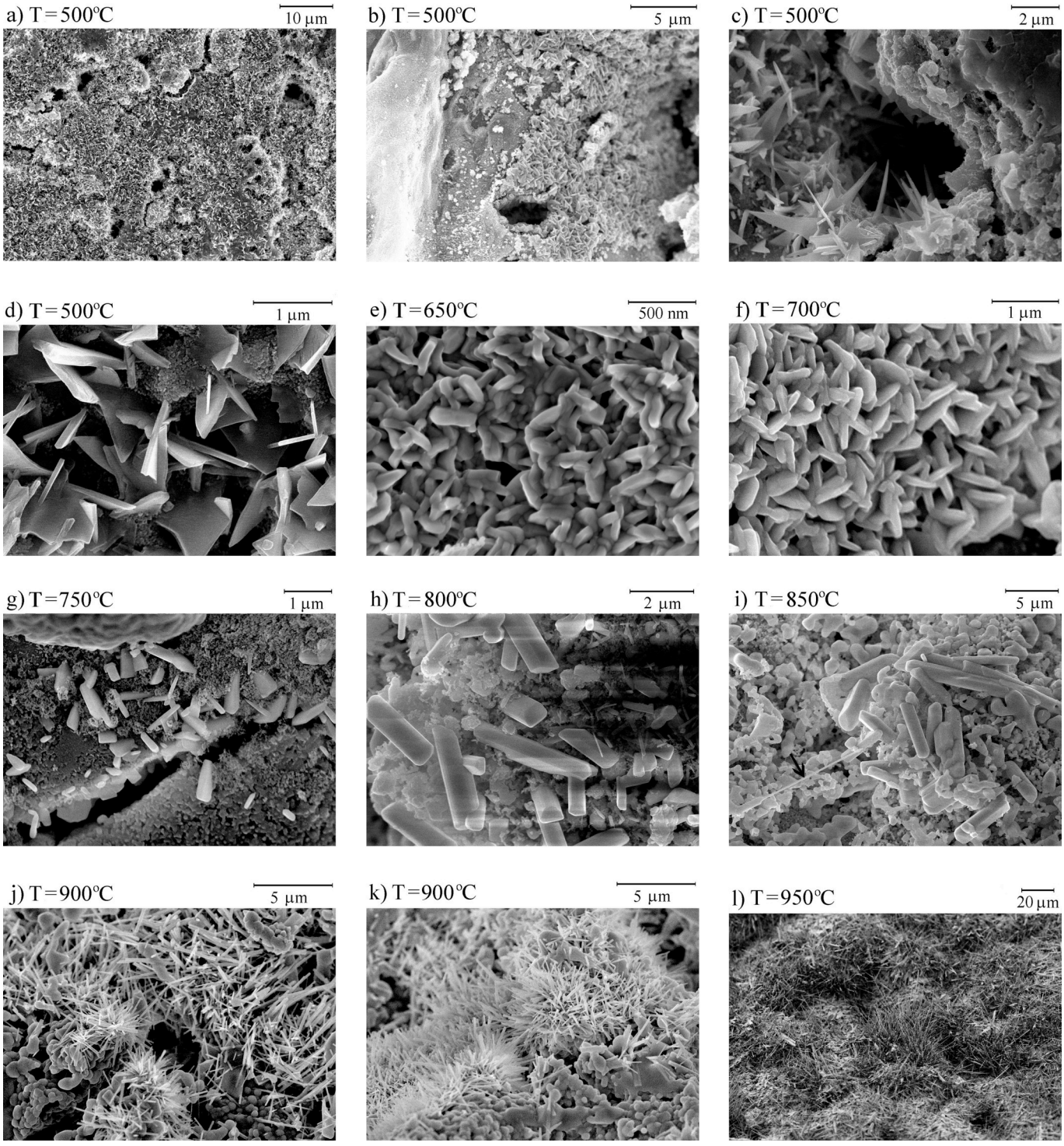

Fig. 2. The examples of micro- and nanoformations on the surface of the samples annealed in air at temperatures of 500 ÷ 950 °C.

prevent surface charging, gold was preliminarily sputtered on the samples. Using the attachment for energy dispersive X-ray spectrum analysis (EDX), we investigated both the average elemental composition of surface areas of 60 × 40 μm and the composition of characteristic formations, focusing the analyzing beam on smaller areas (from 50 × 50 nm and larger). The depth of the analyzed layer was ~ 1 μm. The composition of the surface and that of the characteristic formations were found as average of 3–5 measurements.

The X-ray diffraction (XRD) patterns of the samples with coatings were recorded on a D8 ADVANCE X-ray diffractometer (Germany) in CuK_α radiation. In the course of XRD analysis, the EVA search program was used with the PDF-2 database.

3. Results

3.1. Surface morphology

Fig. 2 shows the surface morphology of PEO-coated sample after impregnation and air annealing at 500 °C for 4 h and the examples of micro- and nanocrystals formed on the surface of the coatings annealed

at different temperatures. Already after annealing at T = 500 °C, the surface is covered with plate micro- and nanocrystals (Fig. 2a–d) with a thickness of ~50 nm and sides of ~0.5 ÷ 1 μm. As was shown in Ref. [44], such nanocrystals are predominantly concentrated in the depressions of the coatings and in the vicinity of the pores. Similar plate nanocrystalls are formed at annealing temperatures equal 650 and 700 °C (Fig. 2e and f). After annealing at T = 750 ÷ 850 °C, rod-shaped elongated crystals are visible on the surface, and their sizes increase with annealing temperature (Fig. 2g–i). After annealing at T = 750 °C their thickness and length are ~100–200 nm and ~1 μm, respectively. Upon T = 850 °C their sized are ~0.5–1 μm and ~5–8 μm. After annealing at T ≥ 900 °C, only whiskers are found on the surface (Fig. 2j-l). Their diameter and length are equal ~200 nm and ~3–5 μm, correspondingly. Thus, the shape and sizes of the crystals formed depend on the annealing temperature.

3.2. Elemental composition

The data on the elemental composition of the surface and crystals at different annealing temperatures are taken from Ref. [44] and given in Table 1. It should be noted, that the coating composition, determined by scanning at least four randomly selected areas of 60 × 40 μm, reflects the average surface composition (total composition), which also includes areas with crystals and pores. The areas of the crystal ensembles were chosen to improve the accuracy of measurements when determining their composition. Areas of size ~50 × 50 nm and more were analyzed, focusing the probe beam on the faces of individual crystals and directing it along the length of the crystal. Nevertheless, taking into account that the analysis depth is ~1 μm, it is impossible to exclude the contribution of the coating layer adjacent to the crystal to the results obtained. In each case, the measurements were carried out for at least five crystals, and the results were averaged.

Note, that the crystals did not contain phosphorus in the entire range of temperatures studied, while phosphorus concentration in the coatings approaches 5 at. %. The presence of carbon can be due both to its incorporation from the electrolyte for PEO (acetate ions) and to the contamination of the surface during sample handling.

Coating composition. With increasing the annealing temperature, nickel content in the coating compositions decreases up to 7.5 at. % at T = 800 °C and increases to 23.8 at. % at T = 900 °C. Simultaneously, the copper concentration falls, especially sharply in the temperature range 700 ÷ 750 °C, and disappears completely at T = 800 °C. The tungsten concentration increases, reaching a maximum (3.7 at. %) at T = 800 °C, and decreases with a further increase in the annealing temperature.

Crystal composition. At T = 750 °C, traces of copper are still found in crystals; at T ≥ 800 °C, copper is not detected in crystals, as on the surface as a whole. That is, the trends in the concentration of copper in coatings and crystals with the annealing temperature are similar. At the same time, at T ≤ 700 °C, the copper content in the crystals is noticeably higher than its average content over the surface. On the contrary, in contrast to the surface composition, the nickel content in the crystals grows with an increase in the annealing temperature, reaching a maximum at T = 850 °C. At the same temperature, the maximum concentration of tungsten is observed in the crystals. The titanium content increases markedly after annealing at T = 900 °C. At the same annealing temperature, tungsten is absent in the crystals.

Comparison of data of Fig. 2 and Table 1 shows that in the same temperature regions there are micro- and nanocrystals of a certain geometric shape. Thus, the annealing temperature affects both the shape and size of the crystals on the surface, and their elemental composition. These facts are clearly presented in the form of the scheme in Fig. 3.

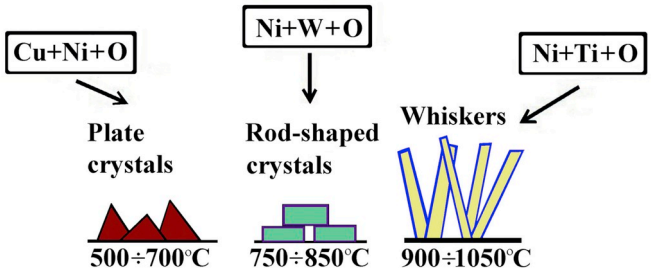

Fig. 3. Schematic representation of crystals on the surface of modified coatings after air annealing in different temperature regions.

3.3. Phase composition

Fig. 4 presents the data of XRD analysis of titanium samples with initial coatings, annealed at required temperatures. Note that, starting from annealing temperatures equal to 850 °C, on flat samples, in contrast to wire samples, partial detachment of the coatings occurred. When the degree of detachment did not exceed 30%, XRD patterns of selected samples with partially delaminated coatings were recorded. With a greater degree of detachment, XRD patterns of the coating materials were did.

In these cases, XRD patterns were taken on selected samples with delaminated areas, occupying no more than 30% of the surface area. When the entire coating was peeled off, an x-ray powder was taken from the (material) of the exfoliated coating.

At all annealing temperatures, the coatings contain titanium dioxide. Up to T = 750 °C, titanium dioxide is present in anatase and rutile modifications. Beginning with T = 850°C, the coatings contain TiO_2 only in rutile modification. The initial coatings (impregnated and annealed at 500 °C) contain nickel and copper oxides. These phases are also present after annealing at 600 and 700 °C. When T = 700 °C, XRD pattern contains reflexes, which we attributed to sodium-titanium phosphate $NaTi_2(PO_4)_3$ and nickel phosphate $Ni_3(PO_4)_2$. When T = 750 °C, nickel and copper oxides are absent in the coating composition, while nickel-titanium phosphate $Ni_{0.5}TiOPO_4$ is found together with $NaTi_2(PO_4)_3$ and $Ni_3(PO_4)_2$. At T = 850 °C, the phase of $NaTi_2(PO_4)_3$ is not recorded, but peaks of $NiWO_4$ appears on XRD patterns. At T = 900 °C, XRD pattern contains the reflexes, which we attributed to $Ni_{2.62}Ti_{0.69}O_4$. When T = 1050 °C, XRD pattern contains only peaks of $Ni_{2.62}Ti_{0.69}O_4$ and phase, which we attributed to $NiTiO_3$.

3.4. The effect of concentration of impregnating solutions

Fig. 5 shows the surface of PEO samples impregnated in 0.5 M Ni$(NO_3)_2$ + 0.5 M Cu$(NO_3)_2$ solutions and in 2 M Ni$(NO_3)_2$ + 2 M Cu$(NO_3)_2$ and annealed. After air annealing at 750 °C of the samples impregnated in the solution with a reduced concentration of nitrates (Fig. 5a and b), the crystals grow locally, tightly filling the pores. Apparently, at such concentrations, the volume of the impregnating solution is sufficient for the formation of crystals only in the pores. In all cases, nanowhiskers grow on the surface of the samples annealed for 1 h at 900 °C (Fig. 5c and d). The higher the concentration of the impregnating solution, the more densely the nanowhiskers fill the surface.

Fig. 6 shows the surface of PEO coatings, not subjected to impregnation, after annealing in air at T = 950 °C. There are no whiskers on

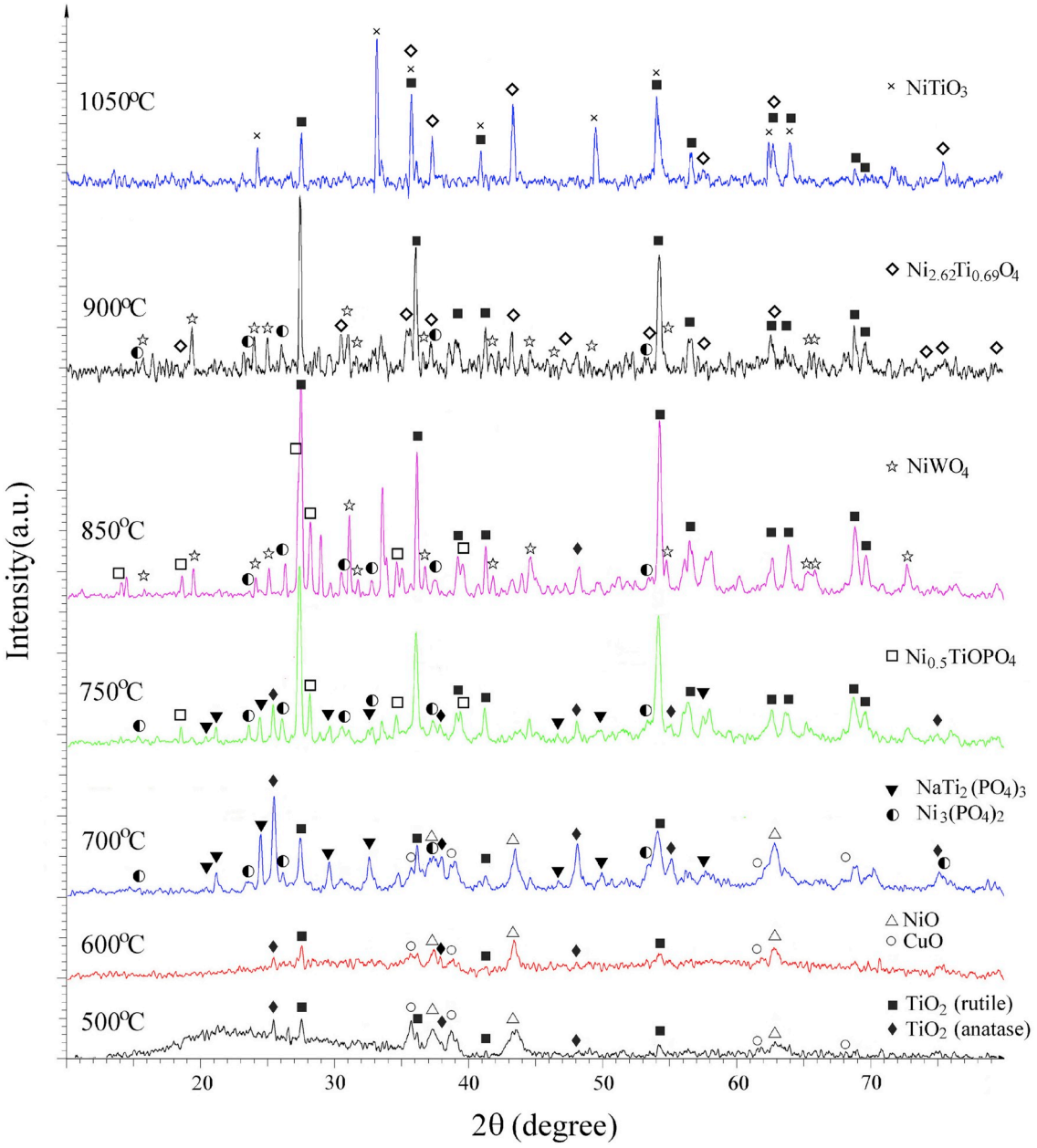

Fig. 4. XRD patterns of the coated samples after air annealing at different temperatures.

the surface. The surface is structured, it consists of microcrystals (Fig. 6a). According to the XRD (Fig. 6b), these are TiO_2 crystals in the rutile modification.

4. Discussion

The initial coatings obtained according to the scheme in Fig. 1, contain decomposition products of the components of the impregnating solution. Thermal decomposition at T = 500 °C should proceed according to the reactions [45]:

$$Ni(NO_3)_2 \rightarrow NiO + 2NO_2 + 1/2O_2 \quad (1)$$

$$Cu(NO_3)_2 \rightarrow CuO + 2NO_2 + 1/2O_2 \quad (2)$$

The impregnating solution contains equimolar concentrations of salts, and, accordingly, close concentrations of nickel and copper are determined in the surface layer (Table 1). According to XRD data (Fig. 4), upon the annealing at 500 °C, the coatings contain nickel and copper oxides formed from the components of impregnating solution by reactions (1) and (2), and titanium oxides (rutile and anatase) from the material of PEO coatings. Note that, prior to the impregnation and annealing operations, the PEO coatings formed in the PBWNiCu electrolyte did not contain crystalline nickel and copper compounds [29]. The halo on XRD pattern in the region of 20–30° (Fig. 4) indicates the compounds in the amorphous or finely crystalline state. Given the composition of electrolyte for PEO, it can be, for example, amorphous phosphates or borates.

In some surface areas of the initial coatings, there are communities of plate nanocrystals with a thickness of ~50 nm and a height of ~500 nm, Fig. 2c and d. Futhermore, such communities are mainly located in the relief depressions and around the pores, Fig. 2b. Considering the data of XRD and elemental analysis, we can conclude that the plate crystals on the surface of the coatings annealed at 500 and 700 °C (Fig. 2d–f) mainly consist of CuO. Obviously, the thermal annealing at these temperatures results in not only the decomposition of

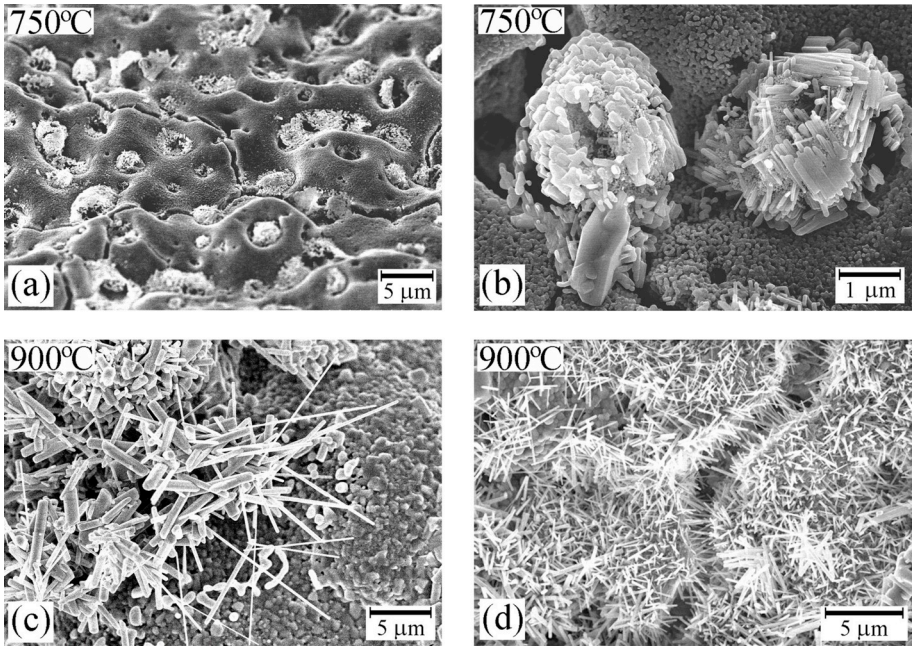

Fig. 5. SEM images of the sample surfaces after their impregnation in the solutions containing 0.5 M $Ni(NO_3)_2$ + 0.5 M Cu $(NO_3)_2$ (a–c) or 2 M $Ni(NO_3)_2$ + 2 M $Cu(NO_3)_2$ (d) followed by annealing for 4 h at 750 °C (a, b) and for 1 h at 900 °C (c, d).

salts as to equations (1) and (2) and removing the gaseous decomposition products from the surface, but also the separation of the components of impregnating solution due to diffusion processes. Apparently, under annealing conditions (T = 500 ÷ 700 °C), due to copper diffusion into the depth and to the surface, communities of Cu-containing plate crystals are formed on the coating surface. Such communities are concentrated in the relief depressions and near the pores, that is, on the surface areas, which are predominantly wetted with an impregnating solution.

Air annealing at 750–800 °C leads to a decrease in the content of nickel and copper, up to the complete disappearance of the latter, and an increase in the content of tungsten in the analyzed surface layer of the coatings (Table 1). Such changes are seem to be associated with the rearrangement of elements on the surface and in the array of the coatings due to diffusion processes. Copper leaves the surface and goes into depth, while tungsten diffuses into the surface layer of the coating. The disappearance of copper on the surface can be associated not only with the processes of diffusion, but also with the sublimation of copper oxide. However, we did not find data on such processes in the available literature. It is only known [46] that due to the volatility of copper oxide, it is rarely used above 1000 °C.

According to XRD data, nickel phosphate $Ni_3(PO_4)_2$ and sodium-titanium phosphate $NaTi_2(PO_4)_3$ are crystallized starting from T = 700 °C. Nickel-titanium phosphate $Ni_{0.5}TiOPO_4$ appears at T = 750 °C. The rod-shaped crystals containing nickel and tungsten are found on the surface (Table 1, Fig. 2g). Since phosphorus is not found in their composition, one can conclude that crystalline phosphates are localized not on the surface, but inside the coating bulk.

After annealing at 850 °C, rod-shaped crystals with a large amount of nickel and tungsten are present on the surface. Given the XRD data (Fig. 4), one can conclude that these are $NiWO_4$ crystals. It is logical to assume that the rod-shaped Ni-, W-containing crystals formed on the surface after annealing at 750–800 °C also contain nickel tungstate.

After annealing at 900–1050°C, ensembles of nanowiskers grow on the surface (Fig. 2j-l, Fig. 5c and d). The growth of whiskers occurs only after additional impregnation. In the absence of an impregnation operation, only rutile microcrystals were found on the surface (Fig. 6). That is, in this case, the components of the impregnating solution play a decisive role. In Ref. [39], the composition of the whiskers was defined as Ni_5TiO_7. Arguments presented in Ref. [47] suggest that the composition of the whiskers is $Ni_5TiO_4(BO_3)_2$. At the same time, the analysis of the obtained XRD pattern of the sample annealed at 900°C (Fig. 7) allows us to conclude that the reflections on the X-ray pattern correspond more to $Ni_{2.62}Ti_{0.69}O_4$ than Ni_5TiO_7 or $Ni_5TiO_4(BO_3)_2$. The elemental composition of whiskers (Table 1) also quite well corresponds to the stoichiometry of the compound $Ni_{2.62}Ti_{0.69}O_4$. Note that, according to Ref. [48], nickel oxide is a rutilizing additive and prevents the formation of nickel titanates in the temperature range of 700–850 °C.

According to the data obtained, it is possible to distinguish three regions of the influence of annealing temperature on the composition and

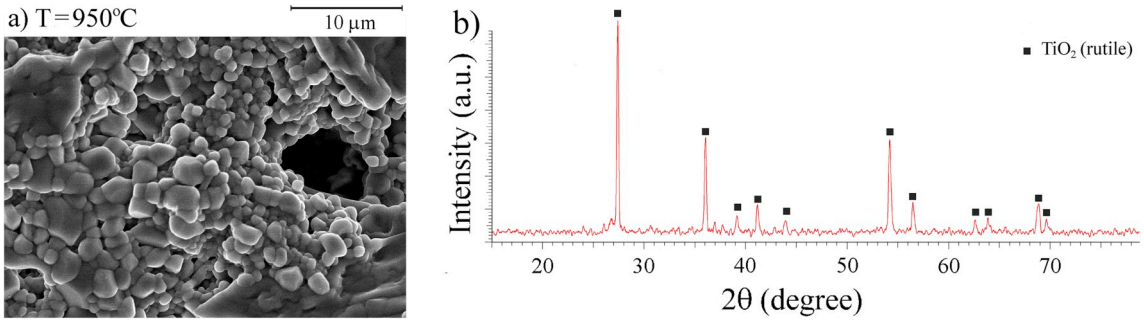

Fig. 6. SEM image (a) and XRD pattern (b) of the non-impregnated sample after air annealing at 950 °C.

Table 1
Effect of annealing temperature on the elemental composition of modified coatings and crystals.

T_{ann}, °C	Elemental composition (C, at. %)														Prevailing shape of crystals
	Coating							Crystals							
	C	O	P	Ti	Ni	Cu	W	C	O	P	Ti	Ni	Cu	W	
500	-	48.8	0.9	4.3	20.4	26.6	-	8.8	31.5	-	3.8	5.5	50.5	-	Plate
700	7.6	49.3	0.7	3.0	18.4	20.7	0.3	11.1	43.6	-	1.8	8.4	35.0	0.1	Plate
750	12.4	59.9	1.9	4.7	14.5	6.0	0.6	26.9	58.2	-	7.3	5.8	1.4	0.4	Rod-shaped
800	10.5	68.5	4.9	4.9	7.5	-	3.7	12.6	63.8	-	7.2	11.1	-	6.8	Rod-shaped
850	28.2	54.0	3.8	5.2	7.7	-	1.1	-	33.4	-	5.1	49.4	-	11.1	Rod-shaped crystals + individual whiskers
900	9.9	54.7	5.1	4.4	23.8	-	2.1	-	57.0	-	11.0	32.0		-	Whiskers

form of micro- and nanocrystals on the coating surfaces (Fig. 3). In region I (T = 500 ÷ 700 °C), crystals are formed from the components of the impregnating solution. In region II (T = 750 ÷ 850°C), the components of the impregnating solution and the electrolyte for PEO take part in the formation of crystals. In region III (T ≥ 900 °C), in addition to the components of the impregnating solution and the electrolyte for PEO, the component of the coating material or metal substrate plays a key role.

The authors of Refs. [39–43] suggest that the growth of $NiWO_4$, $ZnWO_4$, $MnWO_4$, Ni_5TiO_7, $(Ni_{1-x}Co_x)_5TiO_7$ nanocrystals on the surface of PEO coatings as a result of high-temperature annealing is related to the thermal diffusion of the components of impregnating solution and/or electrolyte, which are accumulated in the pores of titania layer on titanium. Moreover, the presence of nuclei is necessary for the growth of the corresponding nanocrystals on the surface of the initial PEO coating.

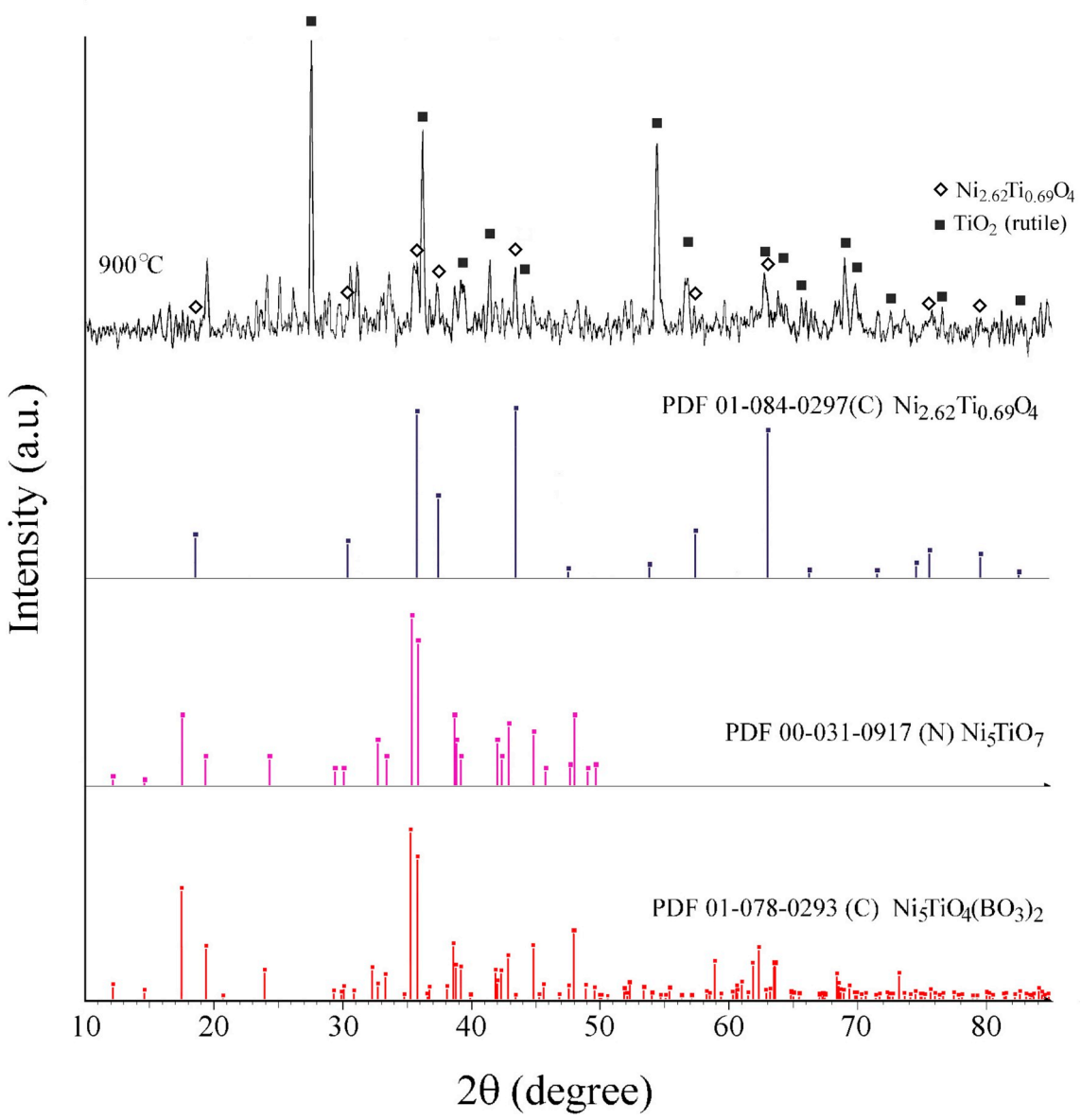

Fig. 7. XRD pattern of the sample annealed at 900 °C. Standard XRD data of $Ni_{2.62}Ti_{0.69}O_4$, Ni_5TiO_7, and $Ni_5TiO_4(BO_3)_2$ are shown as references.

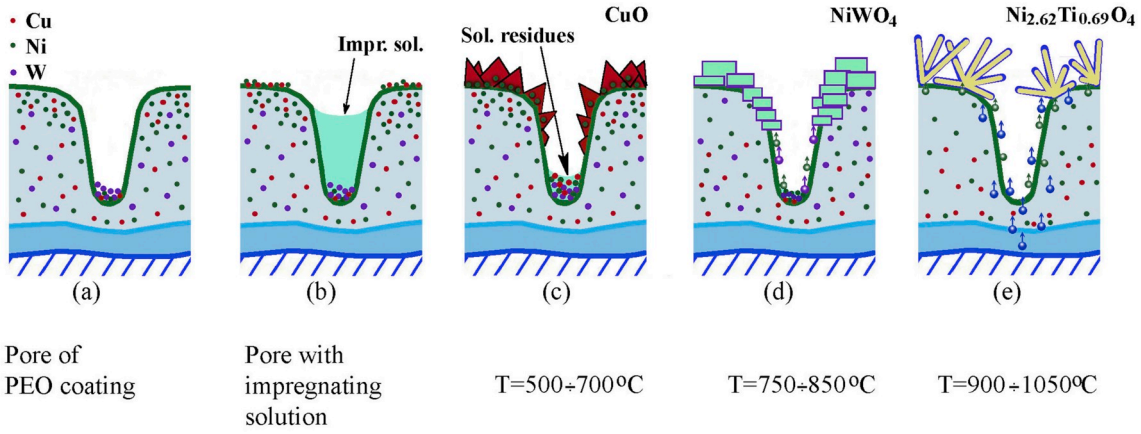

Fig. 8. The proposed scheme of micro- and nanocrystal growth at different annealing temperatures.

Our results do not contradict this assumption. An additional confirmation of this is the predominant formation of crystals in the pores of the coatings at low concentrations of the impregnating solution (Fig. 5a and b). Fig. 8 schematically depicts these processes. Apparently, the impregnating solution selectively wets the surface of the initial sample, mainly near the pores. The pores contain residues of both the impregnating solution and the electrolyte for PEO (Fig. 8b). Annealing at 500 °C leads to dehydration and partial decomposition of the salts on the surface and in the pores. As a result, nanosized plate copper oxide crystals are formed on the surface (Fig. 8c). It is possible that NiO crystallizes in the pores, since crystals with a high nickel content were not found on the surface. A similar situation occurs after annealing at 700 °C.

In the temperature range of 750–850 °C copper is not found on the surface. Apparently, copper diffuses from the surface layer to the depth of the coating. Rod-shaped nickel tungstate crystals are formed on the coating surface, apparently due to the transport of tungsten from the pores to the surface (Fig. 8d). Obviously, the source of tungsten is tungstates, which are present in the pores of PEO coatings. Tungsten transport is observed at temperatures close to the temperature of sublimation of WO_3. As to Ref. [49], sublimation of tungsten trioxide starts at 750 °C and becomes substantial above 900 °C. Under annealing conditions, tungstates decompose to form tungsten trioxide, which moves to the surface, interacts with nickel oxide and forms $NiWO_4$ micro- and nanocrystalls.

Probably, tungsten absence in the surface layer at high annealing temperatures (T = 900 ÷ 1050 °C) is associated with the processes of sublimation of WO_3. Under these conditions, the growth of whiskers of the presumed composition $Ni_{2.62}Ti_{0.69}O_4$ begins initially in the area of pores and cracks (Figs. 2k and 5c).

The nickel necessary for the formation of whiskers can either be located on the surface or be transported from the pores. Since the whiskers of nickel titanate were not found in the absence of the impregnation operation (Fig. 6), then nickel in the array of the PEO layer obviously does not affect their formation. The transport of titanium from the pores can be carried out both from the coating material and from the titanium substrate. It was previously shown that air annealing at T = 850 °C leads to the fact that rutile crystals begin to exit from the pores to the surface of PEO coatings (Fig. 9) [50,51]. The proposed mechanism of the whiskers formation includes high-temperature oxidation of substrate metal due to oxygen diffusion through the pores, counter diffusion of titanium along the walls of the pores to the surface, followed by the formation, growth and extrusion of TiO_2 crystals to the surface. Under such conditions, the thermally stimulated flow of titanium through the pores to the surface leads to its interaction with nickel present in the pores or on the surface with next formation of nickel titanate nanowhiskers (Fig. 8e).

Thus, the mechanism of thermally stimulated changes in the surface architecture of the samples under study can be represented as follows. Despite the washing of samples coated with PEO, there are the forming electrolyte residues in the pores on their surface. As a result of the impregnation, the components of the impregnating solution are concentrated mainly near the pores, in the pores, cracks, as well as in other defective surface areas that are well wetted with this solution. During annealing at 500–700 °C, not only evaporation of water, but also decomposition of nitrates and formation of corresponding oxides (NiO + CuO) occurs on the surface of the samples. Plate crystals of copper oxide are formed in the wetting areas. Perhaps NiO crystallizes in pores or under a layer of CuO crystals. In samples annealed at 750–850 °C, the concentrations of nickel and copper in the surface layer decrease to the complete absence of copper at T = 850 °C, apparently due to diffusion processes. At the same time, due to beginning of WO_3 sublimation from pores containing PEO electrolyte residues, including metal tungstates, the concentration of tungsten on the surface increases and conditions for the growth of $NiWO_4$ crystals are created. Air annealing at 900–1050 °C intensifies the diffusion of titanium from the

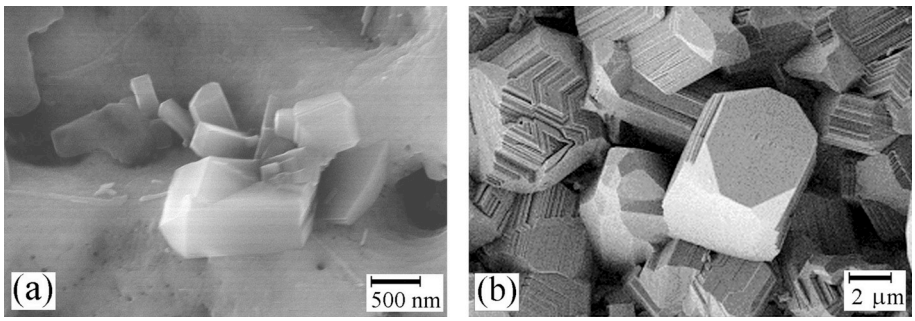

Fig. 9. Growth of rutile crystals in the pores of PEO coatings formed on titanium in the electrolyte containing $Ce_2(SO_4)_3$ + $Zr(SO_4)_2$ according to Refs. [50,51].

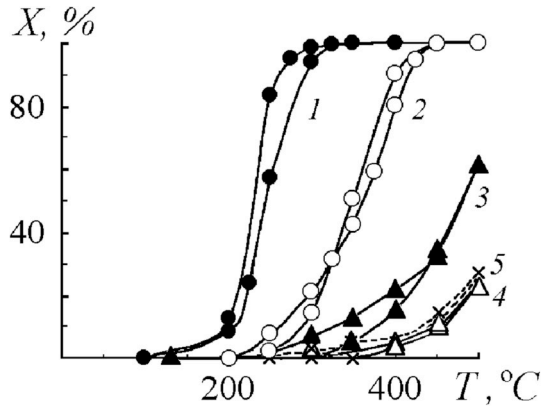

Fig. 10. Temperature dependence of the conversion of CO (X) for modified coatings annealed in air at different temperatures [38].

coating array and the metal substrate along the pore walls onto the surface, as well as the sublimation of WO_3 from the surface, which leads to the formation of $Ni_{2.62}Ti_{0.69}O_4$ whiskers.

The established regularities of changes in the composition and surface morphology with the annealing temperature explain the decrease in the catalytic activity of the samples in the oxidation of CO to CO_2, which was observed in Ref. [38] (Fig. 10). The high activity of the samples annealed at 500 °C correlates with the presence of copper oxide crystals on the surface. The decrease in activity is associated with the restructuring of the surface and the copper diffusion into the depth of the coatings.

It should be noted the similarity of the processes of temperature-stimulated crystal formation in the cases of both applying organic paste to the surface of PEO coatings [36] and impregnation followed by annealing. Taking into account the data of this work and Refs. [31,36–44,50,51], one can expect that annealing at given temperatures of PEO coatings of complex oxide composition, including those additionally modified (impregnation, applying paste or gel, spraying) will be an effective technique for controlling the architecture and composition of the surface at the micro and nanolevels. Moreover, a similar technique may be effective in the case of any porous oxide layers, whose surface is covered by or whose pores are filled with the precursors of compounds of the desired composition.

5. Conclusions

1. Using the techniques of additional impregnation and oxidative annealing at given temperatures, communities of nano- and microcrystals of a certain composition and geometry can be directionally formed on the surface of porous complex oxide coatings on metals. This fact has been demonstrated by the example of NiO + CuO/TiO_2/Ti composites, obtained by plasma electrolytic oxidation with additional impregnation in aqueous solutions of Cu (II) and Ni (II) nitrates. It has been shown that plate CuO crystals based on the components of the impregnating solution are formed on the surface of the composites as a result of annealing in air at T = 500 ÷ 700 °C. At T = 750 ÷ 850°C, rod-shaped crystals $NiWO_4$ grow from the components of the impregnating solution and the electrolyte for PEO. At T ≥ 900 °C, $Ni_{2.62}Ti_{0.69}O_4$ whiskers are formed on the coating surface from the components of the impregnating solution, PEO electrolyte and coating material or metal substrate.
2. The distribution over the surface of nano- and microcrystals growing on the basis of the components of the impregnating solution and the metal-oxide matrix depends on the concentration of the impregnating solutions. Initially, the crystals are concentrated around the pores and cracks of the coating, further spreading over the surface. The formation of $NiWO_4$ crystals correlates with the temperature region of WO_3 sublimation, and the formation of $Ni_{2.62}Ti_{0.69}O_4$ whiskers does with the temperature of intense diffusion of titanium from depth to surface. The pores in the coatings act as the accumulator and source of the components necessary for the formation of micro- and nanocrystals, and as a way to transport titanium from the coating material or metal substrate to the surface.
3. The obtained results and available literature data suggest that oxidative annealing at given temperatures of PEO coatings of complex composition, including additionally modified ones, can be effective for controlling their functional properties by change in the surface architecture and composition on micro and nanolevel. A similar technique may be effective in the case of any porous oxide layers, whose surface is covered by or whose pores are filled with the precursors of compounds of the desired composition.

Acknowledgements

The work was partially supported by grants of RFBR No. 18-03-00418.

References

[1] T.B. Wei, F.Y. Yan, J. Tian, Characterization and wear- and corrosion-resistance of micro arc oxidation ceramic coatings on aluminum alloys, J. Alloy. Compd. 389 (1–2) (2005) 169–176.
[2] Y.L. Cheng, X.Q. Wu, Z.G. Xue, E. Matykina, P. Skeldon, G.E. Thompson, Microstructure, corrosion and wear performance of plasma electrolytic oxidation coatings formed on Ti– 6Al– 4V alloy in silicate-hexametaphosphate electrolyte, Surf. Coat. Technol. 217 (2013) 129–139.
[3] W.H. Song, H.S. Ryu, S.H. Hong, Antibacterial properties of Ag (or Pt)-containing calcium phosphate coating formed by micro-arc oxidation, J. Biomed. Mater. Res. A 88A (1) (2009) 246–254.
[4] O.P. Terleeva, Yu.P. Sharkeev, A.I. Slonova, I.V. Mironov, E.V. Legostaeva, I.A. Khlusov, E. Matykina, P. Skeldon, G.E. Thompson, Effect of microplasma modes and electrolyte composition on micro-arc oxidation coatings on titanium for medical applications, Surf. Coat. Technol. 205 (6) (2010) 1723–1729.
[5] S.F. Tikhov, G.V. Chernykh, V.A. Sadykov, A.N. Salanov, G.M. Alikina, S.V. Tsybulya, V.F. Lysov, Honeycomb catalysts for clean-up of diesel exhausts based upon the anodic-spark oxidized aluminum foil, Catal. Today 53 (4) (1999) 639–646.
[6] F. Patcas, W. Krysmann, Efficient catalysts with controlled porous structure obtained by anodic oxidation under spark-discharge, Appl. Catal. A-Gen. 316 (2) (2007) 240–249.
[7] M.S. Vasil'eva, V.S. Rudnev, L.M. Tyrina, N.B. Kondrikov, V.G. Kuryavyi, E.V. Shchitovskaya, Influence of plasma-electrolytic treatment of titanium on the composition and properties of ruthenium-titanium oxide anodes, Russ. J. Appl. Chem. 77 (12) (2004) 1945–1950.
[8] G.I. Marinina, M.S. Vasilyeva, A.S. Lapina, A.Yu. Ustinov, V.S. Rudnev, Electroanalytical properties of metal-oxide electrodes formed by plasma electrolytic oxidation, J. Electroanal. Chem. 689 (2013) 262–268.
[9] H. Tang, T.Z. Xin, Q. Sun, C.G. Yi, Z.H. Jiang, F.P. Wang, Influence of $FeSO_4$ concentration on thermal emissivity of coatings formed on titanium alloy by micro-arc oxidation, Appl. Surf. Sci. 257 (24) (2011) 10839–10844.
[10] Z.P. Yao, B. Hu, Q.X. Shen, A.X. Niu, Z.H. Jiang, P.B. Su, P.F. Ju, Preparation of black high absorbance and high emissivity thermal control coating on Ti alloy by plasma electrolytic oxidation, Surf. Coat. Technol. 253 (2014) 166–170.
[11] F.Y. Jin, H.H. Tong, J. Li, L.R. Shen, P.K. Chu, Structure and microwave-absorbing properties of Fe-particle containing alumina prepared by micro-arc discharge oxidation, Surf. Coat. Technol. 201 (1–2) (2006) 292–295.
[12] A. Jagminas, R. Ragalevicius, K. Mazeika, J. Reklaitis, V. Jasulaitiene, A. Selskis, D. Baltrunas, A new strategy for fabrication Fe_2O_3/SiO_2 composite coatings on the Ti substrate, J. Solid State Electrochem. 14 (2) (2010) 271–277.
[13] S. Stojadinovic, N. Radic, B. Grbic, S. Maletic, P. Stefanov, A. Pacevski, R. Vasilic, Structural, photoluminescent and photocatalytic properties of TiO_2:Eu^{3+} coatings formed by plasma electrolytic oxidation, Appl. Surf. Sci. 370 (2016) 218–228.
[14] K. Smits, D. Millers, A. Zolotarjovs, R. Drunka, M. Vanks, Luminescence of Eu ion in alumina prepared by plasma electrolytic oxidation, Appl. Surf. Sci. 337 (2015) 166–171.
[15] V.V. Bakovets, O.V. Polyakov, I.P. Dolgovesova, Plasma Electrolytic Anodic Treatment of Metals, Nauka, Novosibirsk, 1991 (in Russian).
[16] P.S. Gordienko, Formation of Coatings on the Anode-Polarized Electrodes in Aqueous Electrolytes at Sparking and Breakdown Potentials, Dal'nauka, Vladivostok, 1996 (in Russian).
[17] P.S. Gordienko, V.S. Rudnev, Electrochemical Formation of Coatings on Aluminum and its Alloys at Sparking and Breakdown Potentials, Dal'nauka, Vladivostok, 1999 (in Russian).
[18] A.L. Yerokhin, X. Nie, A. Leyland, A. Matthews, S.J. Dowey, Plasma electrolysis for surface engineering, Surf. Coat. Technol. 122 (1999) 73–93.
[19] F.C. Walsh, C.T.J. Low, R.J.K. Wood, K.T. Stevens, J. Archer, A.R. Poeton, A. Ryder,

Plasma electrolytic oxidation (PEO) for production of anodised coatings on lightweight metal (Al, Mg, Ti) alloys, Trans. Inst. Metal Finish. 87 (3) (2009) 122–135.
[20] A.G. Rakoch, A.V. Dub, A.A. Gladkova, Anodization of light alloys at different electric modes, Plasma Electrolytic Technology, Staraya Basmannaya, Moscow, 2012(in Russian).
[21] I.V. Suminov, P.N. Belkin, A.V. Apelfeld, V.B. Ludin, B.L. Krit, A.M. Borisov, Plasma Electrolytic Surface Modification of Metals and Alloys 2 Tekhnosfera, Moscow, 2011 (in Russian).
[22] V.S. Rudnev, Multiphase anodic layers and prospects of their application, Protect. Met. 44 (3) (2008) 263–272.
[23] V.S. Rudnev, I.V. Lukiyanchuk, M.S. Vasilyeva, M.A. Medkov, M.V. Adigamova, V.I. Sergienko, Aluminum- and titanium-supported plasma electrolytic multicomponent coatings with magnetic, catalytic, biocide or biocompatible properties, Surf. Coat. Technol. 307 (2016) 1219–1235.
[24] P.I. Butyagin, Ye.V. Khokhryakov, A.I. Mamaev, Microplasma systems for creating coatings on aluminium alloys, Mater. Lett. 57 (2003) 1748–1751.
[25] M.R. Bayati, R. Molaei, H.R. Zargar, A. Kajbafvala, S. Zanganeh, A facile method to grow V-doped TiO_2 hydrophilic layers with nano-sheet morphology, Mater. Lett. 64 (2010) 2498–2501.
[26] I.V. Lukiyanchuk, L.M. Tyrina, V.S. Rudnev, A.Yu. Ustinov, P.M. Nedozorov, M.S. Vasil'eva, Catalytic properties of aluminum/nickel-, copper- containing oxide film compositions, Kinet. Catal. 49 (3) (2008) 439–445.
[27] V.S. Rudnev, Micro- and nano-formations on the surface of plasma electrolytic oxide coatings on aluminum and titanium, Surf. Coat. Technol. 235 (2013) 134–143.
[28] M. Shokouhfar, S.R. Allahkaram, Formation mechanism and surface characterization of ceramic composite coatings on pure titanium prepared by micro-arc oxidation in electrolytes containing nanoparticles, Surf. Coat. Technol. 291 (2016) 396–405.
[29] V.S. Rudnev, L.M. Tyrina, A.Y. Ustinov, S. Vybornova, I.V. Lukiyanchuk, Comparative analysis of the composition, structure, and catalytic activity of the NiO-CuO-TiO_2 on titanium and NiO-CuO-Al_2O_3 on aluminum composites, Kinet. Catal. 51 (2) (2010) 266–272.
[30] M.S. Vasil'eva, V.S. Ru. dnev, The effect of annealing on the composition and morphology of the surface of Ni-containing oxide layers on titanium formed by plasma-electrolytic method, Russ. J. Appl. Chem. 85 (4) (2012) 575–579.
[31] M.S. Vasilyeva, V.S. Rudnev, A.Y. Ustinov, M.A. Tsvetnov, Formation, composition, structure, and catalytic activity in CO oxidation of SiO_2 + TiO_2/Ti composite before and after modification by MnO_x or CoO_x, Surf. Coat. Technol 275 (2015) 84–89.
[32] P.J. Chu, S.Y. Wu, K.C. Chen, J.L. He, A. Yerokhin, A. Matthews, Nano-structured TiO_2 films by plasma electrolytic oxidation combined with chemical and thermal post-treatments of titanium, for dye-sensitised solar cell applications, Thin Solid Films 519 (5) (2010) 1723–1728.
[33] C.C. Tseng, J.L. Lee, Fabrication of bioactive pure Ti by microarc oxidation and hydrothermal treatment methods, Int. J. Electrochem. Sci. 10 (12) (2015) 10232–10245.
[34] H.J. Song, K.H. Shin, M.S. Kook, H.K. Oh, Y.J. Park, Effects of the electric conditions of AC-type microarc oxidation and hydrothermal treatment solution on the characteristics of hydroxyapatite formed on titanium, Surf. Coat. Technol. 204 (14) (2010) 2273–2278.
[35] L.V. Maliy, A.I. Mamaev, V.A. Mamaeva, Structural and optical properties of CdSe/TiO_2 heterostructures produced by high-voltage pulse method, Russ. Phys. J. 60 (10) (2018) 1798–1802.
[36] V.S. Rudnev, M.S. Vasilyeva, M.A. Medkov, P.M. Nedozorov, K.N. Kilin, Fabrication of oxide coatings containing bismuth silicate or bismuth titanate on titanium, Vacuum 122 (2015) 59–65.
[37] I.V. Lukiyanchuk, E.K. Papynov, V.S. Rudnev, V.A. Avramenko, I.V. Chernykh, L.M. Tyrina, A.Yu. Ustinov, V.G. Kuryavyi, D.V. Marinin, Oxide layers with Pd-containing nanoparticles on titanium, Appl. Catal. A-Gen. 485 (2014) 222–229.
[38] V.S. Rudnev, S. Wybornov, I.V. Lukiyanchuk, T. Staedler, X. Jiang, A.Y. Ustinov, M.S. Vasilyeva, Thermal behavior of Ni- and Cu-containing plasma electrolytic oxide coatings on titanium, Appl. Surf. Sci. 258 (22) (2012) 8667–8672.
[39] X. Jiang, L. Zhang, S. Wybornov, T. Staedler, D. Hein, F. Wiedenmann, W. Krumn, V. Rudnev, I. Lukiyanchuk, Highly efficient nanoarchitectured Ni_5TiO_7 catalyst for biomass gasification, ACS Appl. Mater. Interfaces 4 (8) (2012) 4062–4066.
[40] Y.N. Jiang, B. Liu, Z. Zhai, X. Liu, B. Yang, L. Liu, X. Jiang, A general strategy toward the rational synthesis of metal tungstate nanostructures using plasma electrolytic oxidation method, Appl. Surf. Sci. 356 (2015) 273–281.
[41] Y.N. Jiang, B.D. Liu, W.J. Yang, B. Yang, X.Y. Liu, X.L. Zhang, M.A. Mohsin, X. Jiang, New strategy to the in-situ synthesis of single-crystalline $MnWO_4/TiO_2$ photocatalysts for efficient and cyclic photodegradation of organic pollutant, CrystEngComm 18 (2016) 1832–1841.
[42] Y.A. Jiang, B.D. Liu, L.N. Yang, B. Yang, X.Y. Liu, L.S. Liu, C. Weimer, X. Jiang, Size-controllable Ni_5TiO_7 nanowires as promising catalysts for CO oxidation, Sci. Rep. 5 (2015) 14330.
[43] Y.N. Jiang, B.D. Liu, W.J. Yang, L. Yang, S.J. Li, X.Y. Liu, X.L. Zhang, R. Yang, X. Jiang, Crystalline $(Ni_{1-x}Co_x)_5TiO_7$ nanostructures grown in situ on a flexible metal substrate used towards efficient CO oxidation, Nanoscale 9 (32) (2017) 11713–11719.
[44] V.S. Rudnev, I.V. Lukiyanchuk, M.S. Vasilyeva, A.A. Zvereva, Thermally stimulated transformation of the surface nanoarchitecture of Ni-and Cu-doped oxide coatings on titanium, Defect Diffusion Forum 386 (2018) 283–289.
[45] R.A. Lidin, V.A. Molochko, L.L. Andreeva, Reactivity of Inorganic Substances: Handbook. Revised and Augmented Edition, Begell House Inc., New York, 1996.
[46] H. Wayne Richardson (Ed.), Handbook of Copper Compounds and Applications, Marcel Dekker, New York, 1997.
[47] V.B. Nalbandyan, "Ni_5TiO_7" is $Ni_5TiO_4(BO_3)_2$, J. Solid State Chem. 249 (2017) 27–28.
[48] V.V. Viktorov, E.A. Belaya, A.S. Serikov, Phase transformations in the TiO_2-NiO system, Inorg. Mater. 48 (5) (2012) 488–493.
[49] E. Lassner, W.D. Schubert, Tungsten: Properties, Chemistry, Technology of the Element, Alloys, and Chemical Compounds, Kluwer Academic/Plenum Publishers, New York, 1999.
[50] V.S. Rudnev, I.V. Malyshev, I.V. Lukiyanchuk, V.G. Kuryavyi, Composition, surface structure, and thermal behavior of ZrO_2+TiO_2/Ti and ZrO_2+ CeO_x+TiO_2 composites formed by plasma-electrolytic oxidation, Prot. Met. Phys. Chem. Surf. 48 (4) (2012) 455–461.
[51] M.S. Vasilyeva, V.S. Rudnev, F. Wiedenmann, S. Wybomov, T.P. Yarovaya, X. Jiang, Thermal behavior and catalytic activity in naphthalene destruction of Ce-, Zr- and Mn-containing oxide layers on titanium, Appl. Surf. Sci. 258 (2) (2011) 719–726.